Platelet-type 12-lipoxygenase deletion provokes a compensatory 12/15-lipoxygenase increase that exacerbates oxidative stress in mouse islet β cells

Received for publication, December 10, 2018, and in revised form, February 12, 2019 Published, Papers in Press, February 21, 2019, DOI 10.1074/jbc.RA118.007102

Abass M. Conteh[‡§], Christopher A. Reissaus[¶‖], Marimar Hernandez-Perez[¶‖**], Swetha Nakshatri[¶‖**], Ryan M. Anderson[§¶‖**], Raghavendra G. Mirmira[‡§¶‖**], Sarah A. Tersey[¶‖**1], and Amelia K. Linnemann[‡§¶‖**2]**

*From the Departments of [‡]Biochemistry and Molecular Biology, [§]Cellular and Integrative Physiology, and **Pediatrics, [¶]Herman B. Wells Center for Pediatric Research, and [‖]Center for Diabetes and Metabolic Diseases, Indiana University School of Medicine, Indianapolis, Indiana 46202*

Edited by Jeffrey E. Pessin

In type 1 diabetes, an autoimmune event increases oxidative stress in islet β cells, giving rise to cellular dysfunction and apoptosis. Lipoxygenases are enzymes that catalyze the oxygenation of polyunsaturated fatty acids that can form lipid metabolites involved in several biological functions, including oxidative stress. 12-Lipoxygenase and 12/15-lipoxygenase are related but distinct enzymes that are expressed in pancreatic islets, but their relative contributions to oxidative stress in these regions are still being elucidated. In this study, we used mice with global genetic deletion of the genes encoding 12-lipoxygenase (*arachidonate 12-lipoxygenase, 12S type* [*Alox12*]) or 12/15-lipoxygenase (*Alox15*) to compare the influence of each gene deletion on β cell function and survival in response to the β cell toxin streptozotocin. *Alox12*$^{-/-}$ mice exhibited greater impairment in glucose tolerance following streptozotocin exposure than WT mice, whereas *Alox15*$^{-/-}$ mice were protected against dysglycemia. These changes were accompanied by evidence of islet oxidative stress in *Alox12*$^{-/-}$ mice and reduced oxidative stress in *Alox15*$^{-/-}$ mice, consistent with alterations in the expression of the antioxidant response enzymes in islets from these mice. Additionally, islets from *Alox12*$^{-/-}$ mice displayed a compensatory increase in *Alox15* gene expression, and treatment of these mice with the 12/15-lipoxygenase inhibitor ML-351 rescued the dysglycemic phenotype. Collectively, these results indicate that *Alox12* loss activates a compensatory increase in *Alox15* that sensitizes mouse β cells to oxidative stress.

Type 1 diabetes (T1D)[3] is a debilitating chronic disease caused by autoimmunity-mediated destruction of insulin-producing β cells in pancreatic islets. Because of the loss of these cells, individuals who have T1D must rely on exogenous insulin to maintain glucose homeostasis (1). A complex interplay between genetic and environmental factors leads to the autoimmune attack of the β cells, and recent studies suggest that β cell dysfunction may contribute to neoantigen formation, which instigates autoimmunity (2–4). Oxidative stress resulting from an imbalance in favor of oxidants over antioxidants has been suggested as a primary cause of β cell dysfunction in T1D (5–7). Because of their role in the production and release of insulin, β cells generate endogenous reactive species such as hydrogen peroxide, hydroxyl radicals, and peroxynitrites. Paradoxically, β cells possess relatively low antioxidative capacity because of low expression of antioxidant enzymes (8, 9). Interventions that augment antioxidant capacity in mouse models of T1D protect against immunity-mediated β cell destruction (10, 11). Hence, uncovering mechanisms that influence the oxidative stress response in β cells would provide new targets for the treatment of this disease.

Lipoxygenases (LOXs) are lipid-processing enzymes that catalyze the oxygenation of polyunsaturated fatty acids (12). Depending on the specific substrate, lipoxygenases produce a variety of different lipid metabolites that regulate a host of biological functions and disease states (13–15). In mice, the gene *Alox15* encodes for "leukocyte-type" 12-lipoxygenase (known as 12/15-LOX), which catalyzes oxygenation of lipids at carbon 12 or 15 (16, 17). The related gene *Alox12* encodes "platelet-type" 12-lipoxygenase (known as 12-LOX), which oxygenates lipids at carbon 12. Both enzymes catalyze the oxygenation of the polyunsaturated fatty acid arachidonic acid, with 12/15-LOX forming 12- and 15-hydroxyeicosatetraenoic acid (HETE) in a 6:1 ratio, whereas 12-LOX forms only 12-HETE. The activity of 12/15-LOX and its major lipid metabolite, 12-HETE, have been linked to the pathogenesis of T1D. Mice harboring whole-body knockout of *Alox15* show protection from low-dose streptozotocin (STZ)–induced diabetes (18). Likewise, non-obese diabetic mice with whole-body knockout of *Alox15* also show

This work was supported by NIDDK, National Institutes of Health Grants R01 DK105588 and P30 DK097512 (to R. G. M.) and K01 DK102492 and R03 DK115990 (to A. K. L.). The authors declare that they have no conflicts of interest with the contents of this article. The content is solely the responsibility of the authors and does not necessarily represent the official views of the National Institutes of Health.

This article contains Fig. S1.

[1] To whom correspondence may be addressed: 1044 W. Walnut St., R4-325, Indianapolis, IN 46202. Tel.: 317-278-8944; Fax: 317-274-4107; E-mail: stersey@iu.edu.

[2] To whom correspondence may be addressed: 635 Barnhill Dr., MS2031, Indianapolis, IN 46202. Tel.: 317-274-1568; Fax: 317-274-4107; E-mail: aklinnem@iu.edu.

[3] The abbreviations used are: T1D, type 1 diabetes; LOX, lipoxygenase; HETE, hydroxyeicosatetraenoic acid; HODE, hydroxyoctadecadienoic acid; HDHA, hydroxydocosahexaenoic acid; LTB4, leukotriene B4; STZ, streptozotocin; GTT, glucose tolerance test; 4-HNE, 4-hydroxy-2-nonenal; CAT, catalase; ROS, reactive oxygen species; roGFP, redox-sensitive GFP; TNF, tumor necrosis factor; EPA, eicosapentaenoic acid.

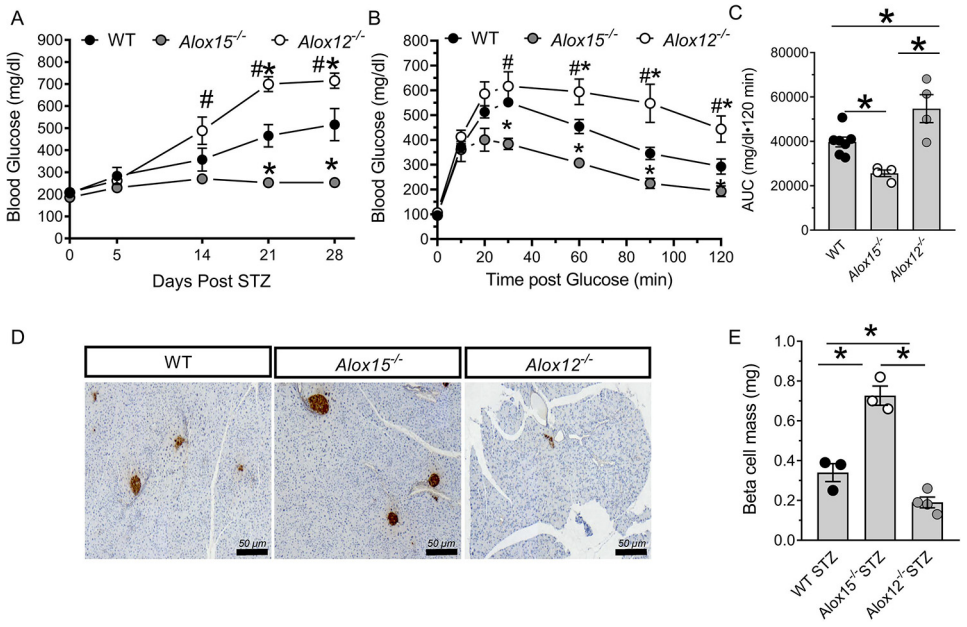

Figure 1. Deletion of *Alox12* exacerbates whereas deletion of *Alox15* protects against STZ-induced diabetes. *A*, random feed blood glucose levels of WT and *Alox12*$^{-/-}$ and *Alox15*$^{-/-}$ mice following the STZ regime. *B*, analysis of glucose tolerance (GTT) in WT, *Alox12*$^{-/-}$, and *Alox15*$^{-/-}$ mice 4 days following the STZ regime. *C*, area under the curve analysis of GTT post STZ. *D*, representative images of insulin immunohistochemistry staining of pancreata for WT, *Alox12*$^{-/-}$, and *Alox15*$^{-/-}$ used for determination of β cell mass. *E*, analysis of β cell mass in WT, *Alox12*$^{-/-}$, and *Alox15*$^{-/-}$ mice following STZ. $n \geq 3$ mice/experimental group for all experiments. *, $p < 0.05$ compared with the WT; #, $p < 0.05$ compared with *Alox15*$^{-/-}$ mice.

protection from the development of T1D (19). This protective effect of loss of *Alox15* is likely due to pancreas expression of the enzyme, as mice with a pancreas-specific deletion of *Alox15* are also protected from low-dose STZ–induced diabetes (18). The specific mechanism underlying this protection has not been identified, but studies have highlighted loss of the lipid metabolite 12-HETE as one possible mechanism. This possibility is supported by evidence that islet exposure to 12-HETE alone can reduce glucose-stimulated insulin secretion and increase islet death (20, 21). In contrast, a role for 12-LOX, which also produces 12-HETE and related eicosanoids, has never been studied in the context of diabetes pathogenesis in the mouse, although it seems to be the primary enzyme in human islets. We reasoned that because both 12-LOX and 12/15-LOX can make 12-HETE and related eicosanoids, loss of *Alox12* should show similar protection as loss of *Alox15*. In this study, we sought to directly compare the effect of loss of *Alox12 versus Alox15* in the setting of T1D.

Results

Deletion of Alox12 exacerbates STZ-induced diabetes, whereas deletion of Alox15 is protective

We sought to assess the metabolic effects of whole-body deletion of the genes encoding 12/15-LOX and 12-LOX (*Alox15* and *Alox12*, respectively) in mice on the C57BL6/J background. As shown in Fig. S1, *A–D*, *Alox15*$^{-/-}$, *Alox12*$^{-/-}$, and their WT control littermate mice at 8 weeks of age exhibited no differences in body weight, glucose tolerance (by intraperitoneal glucose tolerance tests (GTTs)), or β cell mass (by histomorphometric analysis of immunostained pancreata). These results are consistent with prior findings (22–24) that loss of *Alox12* or *Alox15* does not appear to affect the normal development of β cells or whole-body glucose homeostasis.

To assess whether loss of *Alox15* and *Alox12* negatively or positively affects β cell function during the development of diabetes, we leveraged the multiple low-dose STZ model (55 mg/kg body weight STZ intraperitoneally daily for 5 days) to induce diabetes. In this β cell toxicity model, mice develop a T1D-like phenotype with local islet inflammation and consequent hyperglycemia over 4 weeks (24–26). As expected, WT mice developed overt diabetes (blood glucose ≥ 300 mg/dl) within 14 days following STZ injections (Fig. 1*A*, *closed circles*). Consistent with data published previously (19), *Alox15*$^{-/-}$ mice were protected from overt diabetes following STZ (Fig. 1*A*, *gray circles*). In striking contrast, *Alox12*$^{-/-}$ mice exhibited more severe hyperglycemia than WT mice by 14 days following STZ and continuing through the conclusion of the study at 28 days (Fig. 1*A*, *open circles*). GTTs performed 4 days following STZ revealed that *Alox12*$^{-/-}$ mice were significantly more glucose-intolerant than WT and *Alox15*$^{-/-}$ mice, whereas *Alox15*$^{-/-}$ mice showed protection from STZ-induced glucose intolerance compared with WT mice (Fig. 1, *B* and *C*).

We next evaluated β cell mass in STZ-treated mice. As shown in Fig. 1, *D* and *E*, STZ-treated *Alox12*$^{-/-}$ mice exhibited a significant 1.8-fold reduction in β cell mass compared with STZ-treated WT mice. In contrast, β cell mass was more than 2-fold higher in STZ-treated *Alox15*$^{-/-}$ mice compared with STZ-treated WT mice (Fig. 1, *D* and *E*). Together, these data suggest that loss of *Alox12* exacerbates inflammation-induced β cell dysfunction, whereas loss of *Alox15* is protective in this setting.

Deletion of Alox12 exacerbates inflammation-induced oxidative stress in β cells

12-HETE, a lipid product of 12-LOX and 12/15-LOX, is linked to oxidative stress in islets (27). We therefore asked whether oxidative stress in β cells differed in WT, *Alox15*$^{-/-}$,

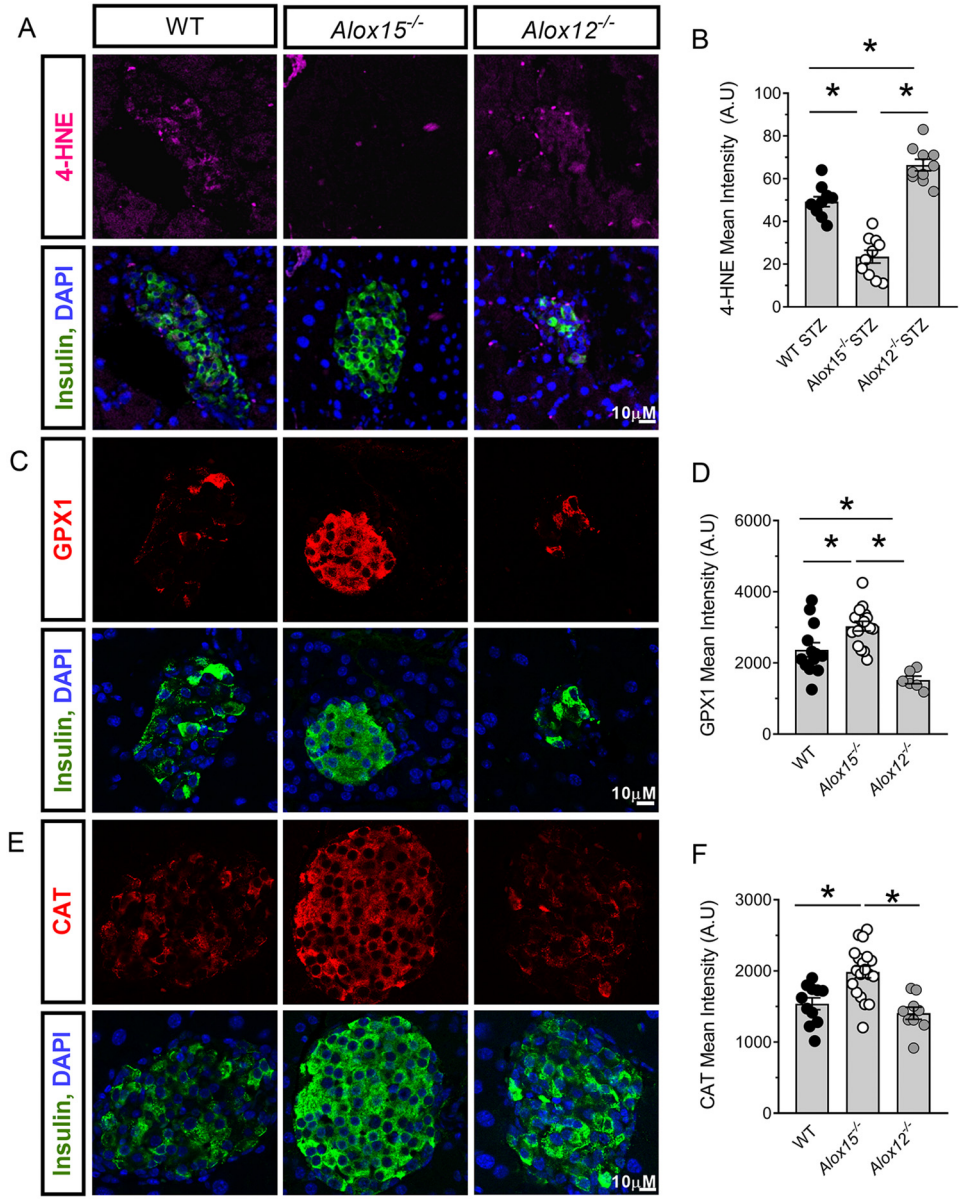

Figure 2. Deletion of *Alox12* exacerbates inflammation-induced oxidative stress in β cells. *A*, representative images of staining for insulin (*green*), the oxidative stress marker 4-HNE (*pink*), and nuclei (*blue*) in WT, *Alox12*$^{-/-}$, and *Alox15*$^{-/-}$ mice following STZ-induced diabetes. *DAPI*, 4′,6-diamidino-2-phenylindole. *B*, quantification of 4-HNE mean intensity in WT, *Alox12*$^{-/-}$, and *Alox15*$^{-/-}$ mice following STZ-induced diabetes. *C*, representative images of staining for insulin (*green*), the oxidative stress marker GPX-1 (*red*), and nuclei (*blue*) in WT, *Alox12*$^{-/-}$, and *Alox15*$^{-/-}$ mice following STZ-induced diabetes. *D*, quantification of GPX-1 mean intensity in WT, *Alox12*$^{-/-}$, and *Alox15*$^{-/-}$ mice following STZ-induced diabetes. *E*, representative images of staining for insulin (*green*), the oxidative stress marker CAT (*red*), and nuclei (*blue*) in WT, *Alox12*$^{-/-}$, and *Alox15*$^{-/-}$ mice following STZ-induced diabetes. *F*, quantification of CAT mean intensity in WT, *Alox12*$^{-/-}$, and *Alox15*$^{-/-}$ mice following STZ induced diabetes. $n \geq 3$ mice/experimental group for all experiments. *, $p < 0.05$; *A.U*, arbitrary units.

and *Alox12*$^{-/-}$ mice after STZ treatment. We examined oxidative stress in tissue sections from STZ-treated control and knockout mice by analysis of islet 4-hydroxynoneal (4-HNE) (28, 29) by immunofluorescence. STZ-treated *Alox15*$^{-/-}$ mice exhibited ~2-fold reduced 4-HNE immunostaining intensity compared with STZ-treated WT mice (Fig. 2, *A* and *B*). However, in agreement with their exacerbated diabetic phenotype, *Alox12*$^{-/-}$ mice exhibited a significant 1.4-fold increase in 4-HNE immunostaining intensity compared with STZ-treated WT mice (Fig. 2, *A* and *B*). To determine whether the opposing effects on oxidative stress observed between *Alox15*$^{-/-}$ and *Alox12*$^{-/-}$ mice could be due to differential production of antioxidant enzymes, we co-immunostained pancreatic sections from STZ-treated WT, *Alox15*$^{-/-}$, and *Alox12*$^{-/-}$ mice for insulin and the antioxidant enzymes GSH peroxidase 1 (GPX1) and catalase (CAT). We observed significant increases in β cell immunostaining intensities of both GPX1 and CAT in *Alox15*$^{-/-}$ mice compared with both WT and *Alox12*$^{-/-}$ mice) (Fig. 2, *C–F*). Conversely, *Alox12*$^{-/-}$ mice showed a significant decrease in β cell GPX1 immunostaining compared with WT and *Alox15*$^{-/-}$ mice (Fig. 2, *C* and *D*). These results suggest that loss of *Alox15* and *Alox12* result in changes in antioxidant protein levels in β cells that may explain their observed effects on β cell oxidative stress.

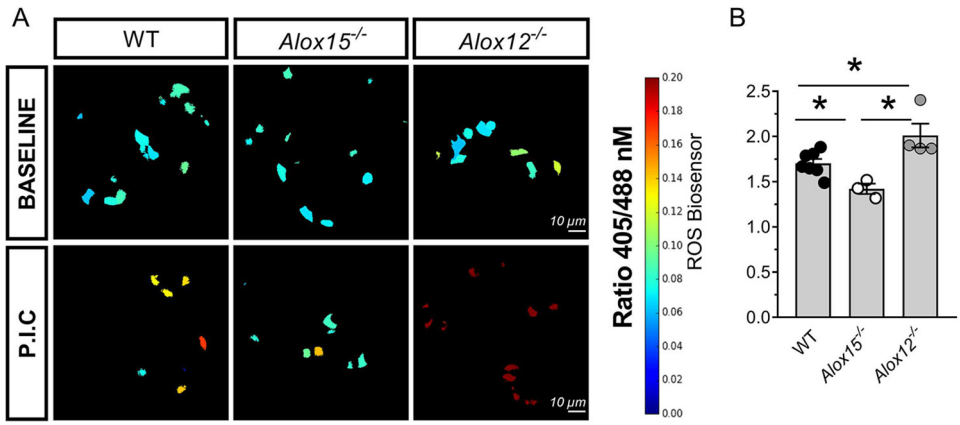

Figure 3. *Alox12* deletion exacerbates reactive oxygen species accumulation in β cells. *A*, ratiometric image of islets from WT, *Alox12*$^{-/-}$, and *Alox15*$^{-/-}$ mice expressing ROGFP2 ROS sensor at baseline and following overnight treatment with a proinflammatory mixture (*P.I.C.*; IL1β, TNFα, and IFNγ). *B*, -fold change of the 405/488 ratio of islets treated with a proinflammatory mixture. $n \geq 3$ mice/experimental group for all experiments. *, $p < 0.05$.

Alox12 deletion exacerbates reactive oxygen species accumulation in β cells

To determine whether the increased oxidative stress was a result of elevated reactive oxygen species (ROS) generation in the islet, we employed the redox biosensor redox-sensitive GFP (roGFP) (30, 31) to measure ROS accumulation dynamically. Islets were transduced with an adenovirus harboring roGFP and then treated for 16 h with a proinflammatory cytokine mixture (IL1-β, TNFα, and IFN-γ) to approximate inflammation-induced oxidative stress. As shown in the representative ratiometric image in Fig. 3*A* and as quantified in Fig. 3*B*, islets from WT mice exhibited an increased redox ratio after cytokine treatment, signifying that cytokines increased ROS. In support of our observations *in vivo*, cytokine-treated *Alox15*$^{-/-}$ islets exhibited significantly less ROS elevation in response to cytokines compared with WT islets. In contrast, cytokines elicited significantly increased ROS in *Alox12*$^{-/-}$ islets compared with WT islets (Fig. 3, *A* and *B*). Collectively, these results suggest that deletion of *Alox15* protects against ROS accumulation, whereas deletion of *Alox12* promotes enhanced oxidative stress.

Alox12 deletion decreases circulating eicosanoid levels in mice

The products of LOXs are biologically active lipid metabolites, and loss of LOXs is expected to alter the levels or ratios of these metabolites, which may account for the effects observed in our mice. To determine the changes in eicosanoid profiles of *Alox12*$^{-/-}$ and *Alox15*$^{-/-}$ mice, we performed LC-MS/MS analysis of key eicosanoids in the circulation of mice. There was no statistically significant difference in circulating levels of 5-HETE, 15-HETE, 13-HODE, 17-HDHA, and LTB4 in *Alox12*$^{-/-}$ and *Alox15*$^{-/-}$ mice compared with WT mice (Table 1). Levels of 12-HEPE were significantly increased in *Alox15*$^{-/-}$ mice compared with controls. There were expected reductions in 12-HETE, which reached statistical significance in *Alox12*$^{-/-}$ mice ($p = 0.02$) and approached significance in *Alox15*$^{-/-}$ mice ($p = 0.06$) compared with WT controls. These data confirm that our knockout mice exhibited reductions in the major 12-LOX and 12/15-LOX metabolite in the circulation.

Alox12 deletion increases STZ-induced oxidative damage through reciprocal up-regulation of Alox15

We next asked how loss of *Alox12* could render mice more sensitive to STZ-induced diabetes. Because *Alox15* and *Alox12* are functionally related, we analyzed the expression of each gene in both *Alox15*$^{-/-}$ and *Alox12*$^{-/-}$ islets and compared them with expression levels in WT controls. Quantitative PCR analysis of *Alox12* mRNA in WT, *Alox15*$^{-/-}$, and *Alox12*$^{-/-}$ islets show the expected decrease in *Alox12*$^{-/-}$ islets and no significant change in *Alox15*$^{-/-}$ islets (Fig. 4*A*). Strikingly, *Alox12*$^{-/-}$ mice exhibited a 28-fold increase in *Alox15* mRNA expression compared with the WT (Fig. 4*B*), suggesting that loss of *Alox12* leads to a compensatory up-regulation of *Alox15* but not vice versa. We hypothesized that the striking reductions in 12-HETE observed in *Alox12*$^{-/-}$ mice (Table 1) might cause a compensatory increase in *Alox15* in this setting, implying that 12-HETE levels might inversely regulate *Alox15*. To test this hypothesis, we incubated Min6 β cells overnight with 100 nM 12-HETE and performed gene expression analysis by quantitative PCR. Treatment with 12-HETE caused a significant reduction in *Alox15* expression compared with the control (Fig. 4*C*), a result that supports our hypothesis. We also sought to determine the effect of 12-HETE on the expression of antioxidant genes. Incubation of Min6 cells with 12-HETE caused a significant decrease in Gpx1 expression (Fig. 4*D*). The expression of Catalase was increased following 12-HETE incubation but was not statistically significant (Fig. 4*E*).

To determine whether the increase in *Alox15* expression contributes to the increased sensitivity of *Alox12*$^{-/-}$ mice to STZ, we employed the 12/15-LOX–specific small-molecule inhibitor ML351 (32). *Alox12*$^{-/-}$ mice treated with ML351 were protected from STZ-induced glucose intolerance compared with vehicle-treated *Alox12*$^{-/-}$ mice (Fig. 4, *F* and *G*). These results suggest that 12/15-LOX levels in *Alox12*$^{-/-}$ mice augment the sensitivity of these mice to STZ-induced dysfunction.

Discussion

LOXs form a family of enzymes that catalyze the oxygenation of cellular polyunsaturated fatty acids to form lipid inflamma-

Table 1

***Alox12* deletion decreases circulating eicosanoid levels in mice**

5-HETE, 12-HETE, 15-HETE, 12-HEPE, 13-HODE, 17-HDHA and LTB4 levels in serum from WT, *Alox12*$^{-/-}$, and *Alox15*$^{-/-}$ mice. $n \geq 3$ mice/experimental group for all experiments. *, $p < 0.05$ versus the WT.

	WT		*Alox15*$^{-/-}$		*Alox12*$^{-/-}$	
	Mean (ng/ml) ± S.E.	*p* value vs. WT	Mean (ng/ml) ± S.E.	*p* value vs. WT	Mean (ng/ml) ± S.E.	*p* value vs. WT
5-HETE	2.88 ± 0.48	-	1.75 ± 0.99	0.270	1.31 ± 0.30	0.264
12-HETE	3433 ± 1143	-	1266 ± 234	0.063	1.01 ± 0.07	0.023*
15-HETE	7.85 ± 2.53	-	3.55 ± 1.60	0.140	2.32 ± 0.81	0.137
12-HEPE	0.89 ± 0.04	-	60.2 ± 6.1	0.001*	Not detected	*
13-HODE	77.33 ± 24.93	-	35.43 ± 8.88	0.140	29.97 ± 5.24	0.140
17-HDHA	515.0 ± 237.6	-	118.2 ± 25.79	0.090	1.46 ± 0.06	0.080
LTB4	9.78 ± 6.50	-	4.032 ± 2.00	0.165	2.36 ± 2.73	0.145

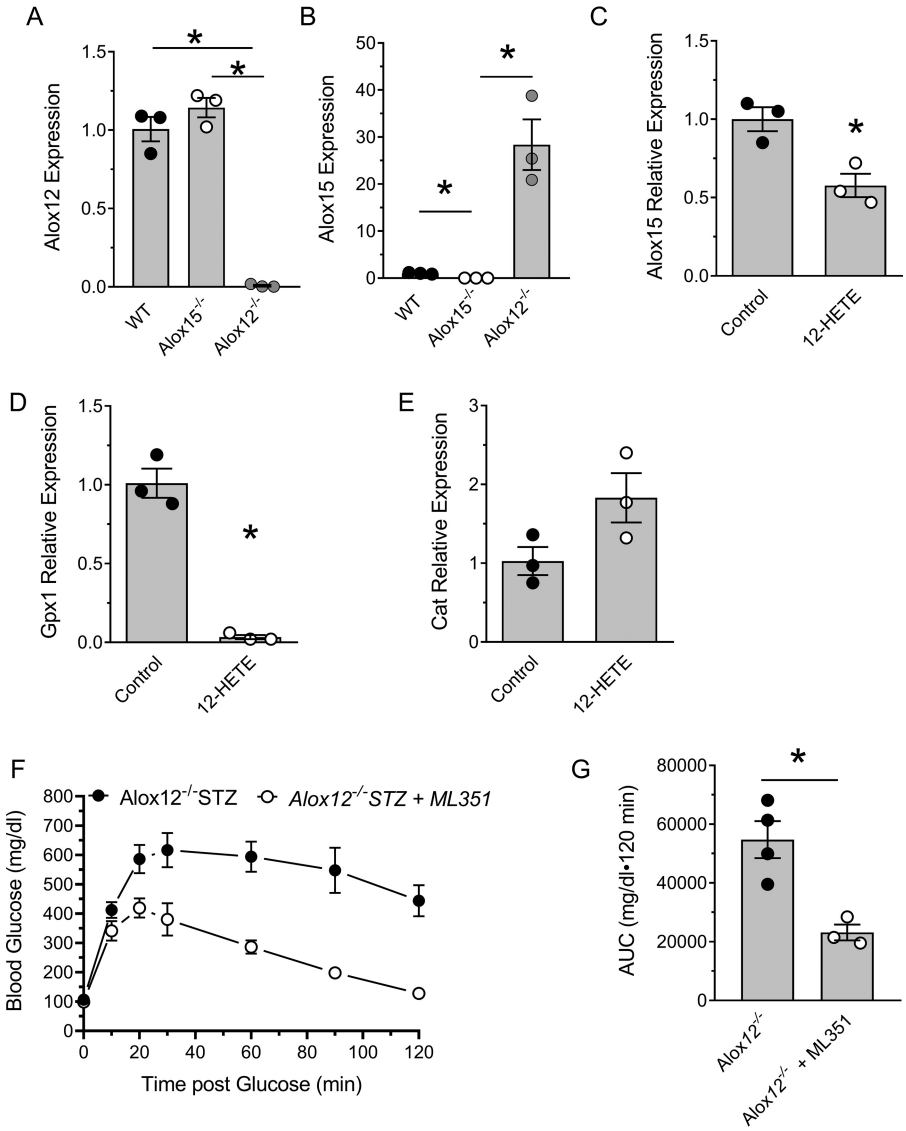

Figure 4. *Alox12* deletion increases STZ-induced oxidative damage through reciprocal up-regulation of *Alox15*. *A*, *Alox12* gene expression in islets from WT, *Alox12*$^{-/-}$, and *Alox15*$^{-/-}$ mice. *B*, *Alox15* gene expression in islets from WT, *Alox12*$^{-/-}$, and *Alox15*$^{-/-}$ mice. *C*, *Alox15* gene expression in Min6 cells following overnight incubation with vehicle or 12-HETE. *D*, Gpx1 gene expression in Min6 cells following overnight incubation with vehicle or 12-HETE. *E*, catalase gene expression in Min6 cells following overnight incubation with vehicle or 12-HETE. *F*, analysis of glucose tolerance (GTT) in vehicle- or ML351-treated *Alox12*$^{-/-}$ mice 4 days following the STZ regime. *G*, area under the curve (*AUC*) analysis of GTTs. $n \geq 3$ mice/experimental group for all experiments. *, $p < 0.05$.

tory mediators (15, 17). LOXs have been shown to contribute to the pathogenesis of T1D and T2D. *Alox12* encodes for 12-LOX (also commonly called platelet-type 12-LOX), which catalyzes the oxygenation of the 12th carbon of its substrates, whereas *Alox15* encodes for 12/15-LOX (also known as leukocyte-type 12-LOX), which oxygenates substrates at either the 12th or 15th carbon (16). 12-LOX–catalyzed oxygenation of arachidonic acid leads to formation of the proinflammatory lipid 12-HETE, and 12/15-LOX forms both 12-HETE and 15-HETE (in a 6:1 ratio) (33). In the setting of diabetes, loss of 12/15-LOX

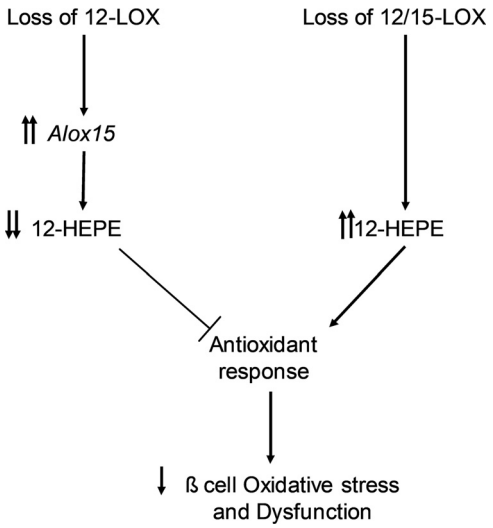

Figure 5. Proposed model of Alox12 *versus* Alox15. Deletion of 12/15-LOX(*Alox15*) leads to a decrease in 12-HETE levels, an increase in 12-HEPE, augmentation of the antioxidant response in β cells during oxidative stress, and increased survival. Deletion of 12-LOX(*Alox12*), on the other hand, causes a compensatory increase in 12/15-LOX(*Alox15*) expression, loss of 12-HEPE production, inhibition of the antioxidant response, and β cell dysfunction.

has been shown to be protective in both STZ and nonobese diabetic mouse models of T1D, effects that have been ascribed to reductions in the levels of 12-HETE (18–20, 33). The proinflammatory actions of 12-HETE may be due to its properties as a lipid peroxide and via its interactions with its receptor Gpr31 (34, 35). Although 12-HETE is also produced by 12-LOX, a role of the *Alox12* gene in β cell oxidative stress during diabetes pathogenesis has not been interrogated. In this study, we interrogated the roles of 12/15-LOX and 12-LOX in the development of oxidative stress in pancreatic islets by studying their respective gene knockouts (*Alox15* and *Alox12*) in the context of T1D models *in vivo* and *in vitro*. Although our data confirm a pro-diabetogenic role of *Alox15*, we found a protective effect for *Alox12*. Our data demonstrate that loss of *Alox12* leads to compensatory hyperactivity of 12/15-LOX encoded by *Alox15* (Fig. 5).

We observed that knockout of either *Alox12* or *Alox15* did not appear to affect β cell mass or glucose homeostasis, findings that are in concordance with prior studies that showed no gross phenotype in unchallenged animals (18, 22). However, a striking and discordant phenotype between the two knockouts was observed when islets of these animals were subjected to proinflammatory stress using the multiple low-dose STZ protocol. STZ is selectively taken up by β cells through the Glut2 transporter and leads to DNA alkylation and eventual cell death (36). Low doses of STZ trigger low-frequency β cell killing, which is exacerbated by macrophage influx, proinflammatory cytokine release, and oxidative stress (37). Under these conditions, prior studies have shown that *Alox15*$^{-/-}$ mice are protected from β cell destruction and hyperglycemia (18). Our results with *Alox15*$^{-/-}$ mice confirm these prior studies but add the vital observation that protection from β cell dysfunction may be caused by reductions in oxidative stress, as judged by reduced immunostaining for 4-HNE accompanied by enhanced immunostaining for the antioxidant enzymes GPX1 and CAT. In contrast, we show that *Alox12*$^{-/-}$ mice exhibit exacerbated hyperglycemia compared with WT controls, with enhanced immunostaining for 4-HNE in β cells accompanied by reduced immunostaining for GPX1 and CAT. Our studies provide the first documented evidence that the enzymes encoded by *Alox15* and *Alox12* display apparently opposing roles in β cell oxidative stress, notwithstanding that both enzymes produce identical major products (12-HETE).

At least two possibilities might be invoked to account for the disparate phenotypes of *Alox15*$^{-/-}$ mice and *Alox12*$^{-/-}$ mice. First, it is possible that the products each enzyme produces and/or their relative ratios can affect the net production of ROS. In this regard, although arachidonic acid and its metabolites are important in cytokine induced β cell dysfunction (38), it is not the only substrate for these enzymes, and the preferential utilization of other key substrates, such as dihomo-γ-linolenic acid or eicosapentaenoic acid (EPA), form products that may be protective (13, 39). Indeed, we observed an increase in circulating levels of the EPA-derived metabolite 12-HEPE in *Alox15*$^{-/-}$ mice that was undetected in the *Alox12*$^{-/-}$ mice. This finding raises the possibility that loss of *Alox15* leads to preferential use of EPA over arachidonic acid as a product. This switch to EPA metabolism has been shown to be protective of β cell function (40). Second, it is possible that the catalytic similarities between the two enzymes might allow one enzyme to compensate to produce the products of the other. We show here that. although no up-regulation of *Alox12* was observed in *Alox15*$^{-/-}$ mice, there was a nearly 30-fold increase in *Alox15* levels in *Alox12*$^{-/-}$ mice. The near-reversal of the diabetogenic phenotype of *Alox12*$^{-/-}$ mice through concurrent pharmacologic inhibition of 12/15-LOX (with ML351) supports the notion that 12/15-LOX activity contributes to the phenotype of these animals. We recognize, however, that we cannot rule out a contribution resulting from the loss of potentially protective lipid products emanating from 12-LOX activity in *Alox12*$^{-/-}$ mice. Based on the lipidomics analysis, we observed a decrease in 12-HETE in the *Alox12*$^{-/-}$ mice. This suggests that the observed detrimental effects observed because of loss of *Alox12*$^{-/-}$ is not caused by an increase in 12-HETE levels. Additionally, we show that 12-HETE inhibits the expression of *Alox15* in Min6 cells. Taken together, the observed decrease in 12-HETE in *Alox12*$^{-/-}$ mice could then lead to the observed up-regulation of *Alox15*.

In conclusion, our data suggest that *Alox15* and *Alox12* play disparate roles in the pathogenesis of β cell oxidative stress and dysfunction. The observation that *Alox15* levels are elevated in *Alox12*$^{-/-}$ islets also highlights a deficiency in our understanding of the regulation of the genes encoding LOX enzymes. As inhibitors of LOX enzymes begin to gain traction for disease modification (32, 41), it will be especially relevant to understand how inhibition of specific enzymes might influence the expression and activities of other related LOXs. Future studies unraveling the effect of complete loss *versus* inhibition of a lipoxygenase enzyme and possible compensatory effects are thus warranted.

Materials and methods

Cells, animals, and procedures

All experiments involving mice were performed with approval from the Indiana University Institutional Animal Care and Use Committee. B6.129S2-Alox12tm1Fun/J (*Alox12*$^{-/-}$) and B6.129S2-Alox15tm1Fun/J (*Alox15*$^{-/-}$) mice were purchased from The Jackson Laboratory and maintained in the Indiana University School of Medicine animal facilities. WT mice were littermates from both *Alox15* and *Alox12* litters. All mice were maintained under pathogen-free conditions. Male mice were injected intraperitoneally daily for 5 consecutive days with saline or streptozotocin at 55 mg/kg/day at 8 weeks of age. A cohort of mice received the 12/15-LOX inhibitor ML351 at 10 mg/kg body weight for 5 days prior, during, and 5 days post-STZ treatment (32). Glucose measurements and intraperitoneal GTTs at 2 g/kg body weight of glucose were performed as described previously (21). At the end of the respective studies, mice were euthanized, serum was collected, and pancreata were harvested and fixed for analysis. Alternatively, mouse islets from both male and female mice were isolated from collagenase-perfused pancreata and cultured in RPMI medium as described previously (42, 43). Islets were handpicked and allowed to recover overnight in complete medium before experimentation. The mouse insulinoma cell line Min6 was maintained in high-glucose DMEM with 15% FBS and 1% penicillin/streptomycin supplemented with 10 mM HEPES and sodium pyruvate and treated with 100 nM 12-HETE for 24 h, followed by RNA isolation using the RNeasy Mini Kit (Qiagen).

Immunohistochemistry, immunofluorescence, and β cell mass

Pancreata were fixed in 4% paraformaldehyde, sectioned, and immunostained for insulin as described previously (44). Pancreata were stained by immunofluorescence using the following primary antibodies: anti-4-HNE antibody (Ab464545, Abcam, 1:100), anti-GPX1 (Santa Cruz), anti-CAT (Santa Cruz), and anti-insulin antibody (A0564, Dako, 1:500). Alexa Fluor 568 donkey anti-rabbit antibody and Alexa Fluor 488 donkey anti-guinea pig antibody were used as secondary antibodies (Invitrogen). Images were acquired using a Zeiss LSM 700 or LSM 800 confocal microscope. 4-HNE immunostainings were quantified by measuring pixel density per insulin-positive cell. β Cell mass was calculated as described previously using at least three pancreas sections 70 μm apart from five pancreata per group (45).

Measurement of β cell redox state

Mouse islets were isolated as described above. After overnight recovery, islets were briefly washed with PBS and distended by incubation with Accutase (STEMCELL Technologies) for 1 min at 37 °C. Accutase was then inactivated, and islets were resuspended in complete islet medium containing serum. Islets were then transduced with the roGFP2 adenovirus for 6 h in complete islet medium. Following transduction, islets were then transferred to virus-free islet medium containing a vehicle or proinflammatory cytokine mixture (5 ng/ml IL-1β, 10 ng/ml TNFα, and 100 ng/ml IFN-γ) for 16 h. Islets were then imaged on a Zeiss LSM 700 confocal microscope. The biosensor was sequentially excited with 405- and 488-nm excitation, and GFP fluorescence was collected and ratioed.

Eicosanoid analysis

Mouse serum collected from WT, *Alox12*$^{-/-}$, and *Alox15*$^{-/-}$ mice was analyzed by the Washington University Metabolomics Core for profiling of eicosanoids (5-HETE, 12-HETE, 8-HETE, 15-HETE, 12-HEPE, 13-HODE, 17-HDHA, and LTB4). Eicosanoids were extracted from 50 μl of serum with 200 μl of methanol containing 2 ng each of deuterated 5-HETE-d_8, 13-HODE-d_4, and LTB4-d_4 as the internal standards. The supernatant was reconstituted with 250 μl of water for MS analyses. Four-point to seven-point calibration standards of all eicosanoids containing the deuterated internal standards were prepared for absolute quantification. The sample analysis was performed with a Shimadzu 20AD HPLC system and a SIL-20AC autosampler coupled to a tandem mass spectrometer (API-6500+, Applied Biosystems) operated in multiple reaction monitoring mode. The negative ion ESI mode was used for detection of these eicosanoids. The plasma extracts were injected in duplicate for data averaging. Data processing was conducted with Analyst 1.6.3 (Applied Biosystems).

Real-time RT-PCR

Reverse-transcribed islet and Min6 RNA was analyzed by real-time PCR using SYBR Green or TaqMan technology. Primers included *Gpx1*, *Cat*, *Alox15*, and *Alox12* (Qiagen). All samples were corrected for input RNA by normalizing to the *Actb* message. All data represent the average of independent determinations from at least three separate mice.

Statistical analysis

All experiments were completed in at least biological triplicates. All data are presented as the mean ± S.E. One-way analysis of variance (with Holm–Sidak's post test) was used for comparisons involving more than two conditions, two-way analysis of variance was used for comparisons with multiple time points, and two-tailed Student's *t* test was used for comparisons involving two conditions. Prism 8 software (GraphPad) was used for all statistical analyses. Statistical significance was assumed at $p < 0.05$.

Author contributions—A. M. C., R. G. M., S. A. T., and A. K. L. conceptualization; A. M. C., C. A. R., and S. A. T. formal analysis; A. M. C., C. A. R., M. H.-P., R. M. A., and S. A. T. validation; A. M. C., C. A. R., M. H.-P., S. N., R. M. A., and S. A. T. investigation; A. M. C., R. G. M., and S. A. T. visualization; A. M. C. and C. A. R. methodology; A. M. C. and A. K. L. writing-original draft; A. M. C., C. A. R., M. H.-P., S. N., R. M. A., R. G. M., S. A. T., and A. K. L. writing-review and editing; R. M. A., R. G. M., and S. A. T. supervision; R. G. M. and A. K. L. resources; R. G. M. and A. K. L. funding acquisition; S. A. T. project administration.

Acknowledgments—We thank Kara Orr, Jennifer Nelson, and Karishma Randhave for technical assistance and the Indiana Diabetes Research Center Islet and Rodent Cores for provision of primary tissues from mice.

References

1. Subramanian, S., Baidal, D., Skyler, J. S., and Hirsch, I. B. (2000) In *Endotext* (De Groot, L. J., Chrousos, G., Dungan, K., Feingold, K. R., Grossman, A., Hershman, J. M., Koch, C., Korbonits, M., McLachlan, R., New, M., Purnell, J., Rebar, R., Singer, F., and Vinik, A., eds.) MDText.com, Inc., South Dartmouth (MA)
2. Redondo, M. J., Jeffrey, J., Fain, P. R., Eisenbarth, G. S., and Orban, T. (2008) Concordance for islet autoimmunity among monozygotic twins. *N. Engl. J. Med.* **359,** 2849–2850 CrossRef Medline
3. Atkinson, M. A., and Eisenbarth, G. S. (2001) Type 1 diabetes: new perspectives on disease pathogenesis and treatment. *Lancet* **358,** 221–229 CrossRef Medline
4. Weir, G. C., and Bonner-Weir, S. (2004) Five stages of evolving β-cell dysfunction during progression to diabetes. *Diabetes* **53,** S16–S21 CrossRef Medline
5. Delmastro, M. M., and Piganelli, J. D. (2011) Oxidative stress and redox modulation potential in type 1 diabetes. *Clin. Dev. Immunol.* **2011,** 593863 Medline
6. Neyestani, T. R., Ghandchi, Z., Eshraghian, M.-R., Kalayi, A., Shariatzadeh, N., and Houshiarrad, A. (2012) Evidence for augmented oxidative stress in the subjects with type 1 diabetes and their siblings: a possible preventive role for antioxidants. *Eur. J. Clin. Nutr.* **66,** 1054–1058 CrossRef Medline
7. Yagishita, Y., Fukutomi, T., Sugawara, A., Kawamura, H., Takahashi, T., Pi, J., Uruno, A., and Yamamoto, M. (2014) Nrf2 protects pancreatic β-cells from oxidative and nitrosative stress in diabetic model mice. *Diabetes* **63,** 605–618 CrossRef Medline
8. Lenzen, S. (2017) Chemistry and biology of reactive species with special reference to the antioxidative defence status in pancreatic β-cells. *Biochim. Biophys. Acta Gen. Subj.* **1861,** 1929–1942 CrossRef Medline
9. Miki, A., Ricordi, C., Sakuma, Y., Yamamoto, T., Misawa, R., Mita, A., Molano, R. D., Vaziri, N. D., Pileggi, A., and Ichii, H. (2018) Divergent antioxidant capacity of human islet cell subsets: a potential cause of β-cell vulnerability in diabetes and islet transplantation. *PLoS ONE* **13,** e0196570 CrossRef Medline
10. Kubisch, H. M., Wang, J., Luche, R., Carlson, E., Bray, T. M., Epstein, C. J., and Phillips, J. P. (1994) Transgenic copper/zinc superoxide dismutase modulates susceptibility to type I diabetes. *Proc. Natl. Acad. Sci. U.S.A.* **91,** 9956–9959 CrossRef Medline
11. Johnson, M. B., Heineke, E. W., Rhinehart, B. L., Sheetz, M. J., Barnhart, R. L., and Robinson, K. M. (1993) MDL 29311: antioxidant with marked lipid- and glucose-lowering activity in diabetic rats and mice. *Diabetes* **42,** 1179–1186 CrossRef Medline
12. Tersey, S. A., Bolanis, E., Holman, T. R., Maloney, D. J., Nadler, J. L., and Mirmira, R. G. (2015) Minireview: 12-lipoxygenase and islet β-cell dysfunction in diabetes. *Mol. Endocrinol.* **29,** 791–800 CrossRef Medline
13. Ackermann, J. A., Hofheinz, K., Zaiss, M. M., and Krönke, G. (2017) The double-edged role of 12/15-lipoxygenase during inflammation and immunity. *Biochim. Biophys. Acta Mol. Cell Biol. Lipids* **1862,** 371–381 CrossRef Medline
14. Kühn, H., and O'Donnell, V. B. (2006) Inflammation and immune regulation by 12/15-lipoxygenases. *Prog. Lipid Res.* **45,** 334–356 CrossRef Medline
15. Mashima, R., and Okuyama, T. (2015) The role of lipoxygenases in pathophysiology: new insights and future perspectives. *Redox Biol.* **6,** 297–310 CrossRef Medline
16. Kuhn, H., Banthiya, S., and van Leyen, K. (2015) Mammalian lipoxygenases and their biological relevance. *Biochim. Biophys. Acta* **1851,** 308–330 CrossRef Medline
17. Newcomer, M. E., and Brash, A. R. (2015) The structural basis for specificity in lipoxygenase catalysis. *Protein Sci.* **24,** 298–309 CrossRef Medline
18. Bleich, D., Chen, S., Zipser, B., Sun, D., Funk, C. D., and Nadler, J. L. (1999) Resistance to type 1 diabetes induction in 12-lipoxygenase knockout mice. *J. Clin. Invest.* **103,** 1431–1436 CrossRef Medline
19. McDuffie, M., Maybee, N. A., Keller, S. R., Stevens, B. K., Garmey, J. C., Morris, M. A., Kropf, E., Rival, C., Ma, K., Carter, J. D., Tersey, S. A., Nunemaker, C. S., and Nadler, J. L. (2008) Nonobese diabetic (NOD) mice congenic for a targeted deletion of 12/15-lipoxygenase are protected from autoimmune diabetes. *Diabetes* **57,** 199–208 CrossRef Medline
20. Ma, K., Nunemaker, C. S., Wu, R., Chakrabarti, S. K., Taylor-Fishwick, D. A., and Nadler, J. L. (2010) 12-Lipoxygenase products reduce insulin secretion and β-cell viability in human islets. *J. Clin. Endocrinol. Metab.* **95,** 887–893 CrossRef Medline
21. Zhou, Y. P., Teng, D., Dralyuk, F., Ostrega, D., Roe, M. W., Philipson, L., and Polonsky, K. S. (1998) Apoptosis in insulin-secreting cells: evidence for the role of intracellular Ca^{2+} stores and arachidonic acid metabolism. *J. Clin. Invest.* **101,** 1623–1632 CrossRef Medline
22. Tersey, S. A., Maier, B., Nishiki, Y., Maganti, A. V., Nadler, J. L., and Mirmira, R. G. (2014) 12-Lipoxygenase promotes obesity-induced oxidative stress in pancreatic islets. *Mol. Cell. Biol.* **34,** 3735–3745 CrossRef Medline
23. Nunemaker, C. S., Chen, M., Pei, H., Kimble, S. D., Keller, S. R., Carter, J. D., Yang, Z., Smith, K. M., Wu, R., Bevard, M. H., Garmey, J. C., and Nadler, J. L. (2008) 12-Lipoxygenase-knockout mice are resistant to inflammatory effects of obesity induced by Western diet. *Am. J. Physiol. Endocrinol. Metab.* **295,** E1065–75 CrossRef Medline
24. Johnson, E. N., Nanney, L. B., Virmani, J., Lawson, J. A., and Funk, C. D. (1999) Basal transepidermal water loss is increased in platelet-type 12-lipoxygenase deficient mice. *J. Invest. Dermatol.* **112,** 861–865 CrossRef Medline
25. Ward, D. T., Yau, S. K., Mee, A. P., Mawer, E. B., Miller, C. A., Garland, H. O., and Riccardi, D. (2001) Functional, molecular, and biochemical characterization of streptozotocin-induced diabetes. *J. Am. Soc. Nephrol.* **12,** 779–790 Medline
26. Lukić, M. L., Stosić-Grujicić, S., and Shahin, A. (1998) Effector mechanisms in low-dose streptozotocin-induced diabetes. *Dev. Immunol.* **6,** 119–128 CrossRef Medline
27. Weaver, J. R., Holman, T. R., Imai, Y., Jadhav, A., Kenyon, V., Maloney, D. J., Nadler, J. L., Rai, G., Simeonov, A., and Taylor-Fishwick, D. A. (2012) Integration of pro-inflammatory cytokines, 12-lipoxygenase and NOX-1 in pancreatic islet β cell dysfunction. *Mol. Cell Endocrinol.* **358,** 88–95 CrossRef Medline
28. Zarkovic, K., Jakovcevic, A., and Zarkovic, N. (2017) Contribution of the HNE-immunohistochemistry to modern pathological concepts of major human diseases. *Free Radic. Biol. Med.* **111,** 110–126 CrossRef Medline
29. Esterbauer, H., Schaur, R. J., and Zollner, H. (1991) Chemistry and biochemistry of 4-hydroxynonenal, malonaldehyde and related aldehydes. *Free Radic. Biol. Med.* **11,** 81–128 CrossRef Medline
30. Lismont, C., Walton, P. A., and Fransen, M. (2017) Quantitative monitoring of subcellular redox dynamics in living mammalian cells using RoGFP2-based probes. *Methods Mol. Biol.* **1595,** 151–164 CrossRef Medline
31. Müller, A., Schneider, J. F., Degrossoli, A., Lupilova, N., Dick, T. P., and Leichert, L. I. (2017) Systematic *in vitro* assessment of responses of roGFP2-based probes to physiologically relevant oxidant species. *Free Radic. Biol. Med.* **106,** 329–338 CrossRef Medline
32. Hernandez-Perez, M., Chopra, G., Fine, J., Conteh, A. M., Anderson, R. M., Linnemann, A. K., Benjamin, C., Nelson, J. B., Benninger, K. S., Nadler, J. L., Maloney, D. J., Tersey, S. A., and Mirmira, R. G. (2017) Inhibition of 12/15-lipoxygenase protects against β cell oxidative stress and glycemic deterioration in mouse models of type 1 diabetes. *Diabetes* **66,** 2875–2887 CrossRef Medline
33. Prasad, K.-M., Thimmalapura, P.-R., Woode, E. A., and Nadler, J. L. (2003) Evidence that increased 12-lipoxygenase expression impairs pancreatic β cell function and viability. *Biochem. Biophys. Res. Commun.* **308,** 427–432 CrossRef Medline
34. Zhang, X.-J., Cheng, X., Yan, Z.-Z., Fang, J., Wang, X., Wang, W., Liu, Z.-Y., Shen, L.-J., Zhang, P., Wang, P.-X., Liao, R., Ji, Y.-X., Wang, J.-Y., Tian, S., Zhu, X.-Y., *et al.* (2018) An ALOX12–12-HETE–GPR31 signaling axis is a key mediator of hepatic ischemia–reperfusion injury. *Nat. Med.* **24,** 73–83 Medline
35. Guo, Y., Zhang, W., Giroux, C., Cai, Y., Ekambaram, P., Dilly, A.-K., Hsu, A., Zhou, S., Maddipati, K. R., Liu, J., Joshi, S., Tucker, S. C., Lee, M.-J., and Honn, K. V. (2011) Identification of the orphan G protein-coupled recep-

tor GPR31 as a receptor for 12-*S*-hydroxyeicosatetraenoic acid. *J. Biol. Chem.* **286,** 33832–33840 CrossRef Medline

36. Eleazu, C. O., Eleazu, K. C., Chukwuma, S., and Essien, U. N. (2013) Review of the mechanism of cell death resulting from streptozotocin challenge in experimental animals, its practical use and potential risk to humans. *J. Diabetes Metab. Disord.* **12,** 60 CrossRef Medline
37. Nahdi, A. M. T. A., John, A., and Raza, H. (2017) Elucidation of molecular mechanisms of streptozotocin-induced oxidative stress, apoptosis, and mitochondrial dysfunction in Rin-5F pancreatic β-cells. *Oxid. Med. Cell. Longev.* CrossRef
38. Lei, X., Bone, R. N., Ali, T., Zhang, S., Bohrer, A., Tse, H. M., Bidasee, K. R., and Ramanadham, S. (2014) Evidence of contribution of iPLA2β-mediated events during islet β-cell apoptosis due to proinflammatory cytokines suggests a role for iPLA2β in T1D development. *Endocrinology* **155,** 3352–3364 CrossRef Medline
39. Ikei, K. N., Yeung, J., Apopa, P. L., Ceja, J., Vesci, J., Holman, T. R., and Holinstat, M. (2012) Investigations of human platelet-type 12-lipoxygenase: role of lipoxygenase products in platelet activation. *J. Lipid Res.* **53,** 2546–2559 CrossRef Medline
40. Neuman, J. C., Schaid, M. D., Brill, A. L., Fenske, R. J., Kibbe, C. R., Fontaine, D. A., Sdao, S. M., Brar, H. K., Connors, K. M., Wienkes, H. N., Eliceiri, K. W., Merrins, M. J., Davis, D. B., and Kimple, M. E. (2017) Enriching islet phospholipids with eicosapentaenoic acid reduces prostaglandin E2 signaling and enhances diabetic β-cell function. *Diabetes* **66,** 1572–1585 CrossRef Medline
41. Hu, C., and Ma, S. (2018) Recent development of lipoxygenase inhibitors as anti-inflammatory agents. *Medchemcomm.* **9,** 212–225 CrossRef Medline
42. Marasco, M. R., Conteh, A. M., Reissaus, C. A., Cupit, J. E., 5th, Appleman, E. M., Mirmira, R. G., and Linnemann, A. K. (2018) Interleukin-6 reduces β-cell oxidative stress by linking autophagy with the antioxidant response. *Diabetes* **67,** 1576–1588 CrossRef Medline
43. Stull, N. D., Breite, A., McCarthy, R., Tersey, S. A., and Mirmira, R. G. (2012) Mouse islet of Langerhans isolation using a combination of purified collagenase and neutral protease. *J. Vis. Exp.* **7,** 4137 CrossRef Medline
44. Maier, B., Ogihara, T., Trace, A. P., Tersey, S. A., Robbins, R. D., Chakrabarti, S. K., Nunemaker, C. S., Stull, N. D., Taylor, C. A., Thompson, J. E., Dondero, R. S., Lewis, E. C., Dinarello, C. A., Nadler, J. L., and Mirmira, R. G. (2010) The unique hypusine modification of eIF5A promotes islet β cell inflammation and dysfunction in mice. *J. Clin. Invest.* **120,** 2156–2170 CrossRef Medline
45. Cabrera, S. M., Colvin, S. C., Tersey, S. A., Maier, B., Nadler, J. L., and Mirmira, R. G. (2013) Effects of combination therapy with dipeptidyl peptidase-IV and histone deacetylase inhibitors in the non-obese diabetic mouse model of type 1 diabetes. *Clin. Exp. Immunol.* **172,** 375–382 CrossRef Medline